IVYSPRING INTERNATIONAL PUBLISHER

JOURNAL OF CANCER

2026; 17(8): 1408-1418. doi: 10.7150/jca.134767

Research Paper

GPCRs interaction with LGR5: Implications to cancer stemness

Jeetendra K Nag[1], Ganesh Subedi [1,2], Tatyana Rudina[3], Rachel Bar-Shavit[3,✉]

1. Department of Heart, Blood and Kidney Research, Cleveland, Clinic Research, Cleveland, OH 44195 USA.
2. Department of Chemistry, Cleveland State University, Cleveland, OH 44115 USA.
3. Sharett Institute of Oncology, Hadassah-Hebrew University, Medical Center, Jerusalem, Israel.

✉ Corresponding author: Rachel Bar-Shavit; rachelbar@ekmd.huji.ac.il.

Received: 2026.03.20; Accepted: 2026.05.26; Published: 2026.07.20

Abstract

Background/Objectives: The central role of G-protein coupled receptors (GPCRs) in tumor biology is becoming acknowledged. Yet their involvement in cancer stem cells (CSCs) niche is unknown. Molecular mechanisms of CSCs allow self-formation capacity, resistance to chemotherapy and immune therapy.

Methods: Western blots, Co-immunoprecipitation (co-IP) analysis, RT-PCR, *Lef*/*Tcf* luciferase activity and Alpha Fold3 HANDDOCK v2.4 protein-protein docking interactions.

Results: It is demonstrated that protease-activated receptor 4 (PAR_4) induces β-catenin levels, co-associates with LRP6 coreceptor and promotes DVL nuclear translocation. PAR_4 induced β-catenin transcriptional activity is shown by TOP*flash* luciferase assay and enhanced downstream target genes levels. Significantly, PAR_4 co-binds leucine-rich repeat-containing G protein-coupled receptor 5 (LGR5) as determined by co-IP and protein-protein docking analyses. We show also that another GPCR namely, GPR25 specifically expressed in the gastrointestinal tract cells, elicits β-catenin stabilization and co associates with LGR5.

Conclusions: As was previously shown for PAR_2 also PAR_4 and GPR25 elicit β-catenin stabilization and they co-link with LGR5. We propose that GPCRs that potently induce β-catenin stabilization are potentially involved in the regulation of CSCs niche. Our data may provide future directions for potential partners in the cancer stem cell niche.

Keywords: cancer stem cells (CSCs), protease-activated receptors (PARs), LGR5, G-protein coupled receptors (GPCRs), β-catenin stabilization

Introduction

Cancer stem cells (CSCs) are the cornerstone in cancer biology constantly driven by molecular mechanisms that foster self-renewal capacity. CSCs have been linked with tumor growth, metastasis, and relapses; therefore, they are attractive candidates for cancer therapy [1]. Due to their powerful self-renewal capability, CSCs continuously initiate tumor cell proliferation assisting tumor growth state. Like the adult stem cells, high degree plasticity takes place in CSCs which depends on tight interactions with the tumor microenvironment [1-4]. Notably, CSCs are a self-autonomous entity governed by the powerful Wnt/β-catenin pathway, oncogenes mutations and/or their overexpression pattern. Yet the dynamics of plasticity are largely determined by environmental signs [5-8]. Proteolysis remodeling of the extracellular matrix tumor microenvironment induces cancer cell invasion and metastasis [9]. Consequently, the disseminated tumor front is guided by enriched population of CSCs and proteases [8,10]. Leucine-rich repeat-containing G protein-coupled receptor 5 (LGR5), a cancer stem cell marker is highly expressed at the origin of a tumor. LGR5, a seven transmembrane domain receptor, is a member of the G-protein coupled receptor (GPCR) family. In fact, LGR5 is a Wnt target gene expressed for example, at the crypt base of small intestines [4, 11-13]. Along with its homolog proteins, LGR4 and LGR6, LGR5 form a family of receptors that

are activated by R-spondins [14, 15]. As the role of GPCRs in cancer biology is acknowledged, their involvement in CSC regulation is unknown. Protease activated receptors (PARs) are sensitive sensors of proteases that are stored anchored within the tumor microenvironment. Mammalian PARs form a family of four members; PAR_{1-4} that belongs to the large family of GPCRs. These receptors are uniquely activated via proteolytic cleavage at their N-terminal portion and the exposure of hindered internal ligands. We as also others have reported a central role for PARs in tumor biology [16-18]. We demonstrated a potent stabilization and high β-catenin levels (as compared to their wild type (*wt*) age matched tissues of mammary glands) in a transgenic mouse line directed to overexpress *Par1/f2r* in the mouse mammary fat pads [19]. In fact, both $PAR_{1\&2}$ have been found to be potent inducers of β-catenin stabilization, leading to β-catenin transcriptional activity and increased levels of target gene signature. Noticeably, PAR induced β-catenin stabilization takes place regardless of the presence of Wnts as demonstrated by Wnt or frizzled (FZD) inhibitors. These are Porcupine (e.g., LGK974), the Wnt inhibitor or sFRP [secreted frizzleds (FZDs)-related protein] that acts to bind the FZD extracellular portion at the Wnt binding site, thus neutralizing FZDs, Wnts receptors [20]. PARs potently induce β-catenin stabilization in the presence of Porcupine or sFRP. As was demonstrated for Wnt induced β-catenin stabilization, PAR_2 recruits LRP6 as a co receptor then induces the translocation of cytoplasmic disheveled (DVL) to the cell nuclei [21]. Up till now primary regulators that control PAR-induced β-catenin path are understudied. Posttranslational regulation of PAR_2 in colon cancer growth and development have demonstrated the negative impact of Ring Finger Protein 43 (RNF43) on PAR_2 expression levels and consequently on PAR_2 induced colon cancer development.

We have demonstrated that RNF43 degrades cell surface PAR_2 levels through ubiquitination. This PAR_2 degradation is rescued by LGR5 and R-spondin. Overall, this mode of PAR_2 regulation is comparable to FZDs degradation by RNF43, liberated by R-spondin-LGR5 [20]. In the present manuscript we provide evidence showing that PAR_4 oncogene [18] is a powerful inducer of β-catenin stabilization like PAR_1 and PAR_2. In addition, it is demonstrated that PAR_4 co associates with the cancer stem cell marker - LGR5. Along this line of evidence, we present data that another cancer GPCR; GPR25 is highly expressed in the gastrointestinal (GI) tract. GPR25 is a poorly studied orphan receptor. We demonstrate that GPR25 induces β-catenin stabilization and TOP*flash* transcriptional activity. Similarly, it co associates with LGR5. Collectively, our data indicate that PAR_4 and GPR25 induce the stabilization of β-catenin and are linked with the cancer stem cell; LGR5. Implications of our findings can be best implemented in colon cancer, mainly driven by the β-catenin stabilization path.

Material and Methods

Cell and culture conditions

HEK293, HU, HCT-116, HT-29, RKO, MDA 231, MCF-7, A549, HTR8, Panc-1(obtained from the American Type Culture Collection) were grown in DMEM, supplemented with 1 mM L-glutamine, 50 μg/mL streptomycin,50 U/mL penicillin (GIBCO-BRL, Gaithersburg, USA) and 10% fetal calf serum (Biological Industries, Israel). Cells were maintained in a humidified incubator with 8% CO2 at 37^0C.

Plasmids and reagents

Human PAR_2 (*Par2/f2rl1*) plasmid was kindly provided by Dr. Morley D. Hollenberg (Faculty of Medicine, University of Calgary, Alberta, Canada). The *flg*-β-catenin was kindly provided by Dr. Ben-Neria (Hebrew University, Jerusalem). The plasmid encoding LGR5 was kindly provided by Dr. Joshua C. Snyder (Duke University Medical Center, USA). *pBJ-FLAG-Par4 (cat #53231* and *gpr25* were purchased (Addgene, MA USA). Plasmids purchased from Addgene were sequenced to confirm the absence of undesirable mutations. Details of plasmids are available on request.

Cell transfections and PAR activation

Cells grown to 70%−80% confluency were transfected with 0.5-1μg amount of plasmid DNA using PEI transfection reagent (Polysciences, Warrington, PA, USA) according to the manufacturer's instructions. Cells were collected 48h after transfection and protein lysates or RNA were prepared. To activate PAR_2, a synthetic peptide SLIGKV (purchased from GenScript; Piscataway, USA) was used. For PAR_4 activation, AYPGKF peptide (GenScript; Piscataway, USA) were used.

RNA isolation and RT-PCR

RNA was isolate using GeneElute™ Mammalian Total RNA Miniprep kit (Sigma-Aldrich, Israel; Cat no. RTN70-1KT) according to the manufacturer's instructions. After reverse transcription of 1μg total RNA by oligo (dT) priming, cDNA was amplified using Taq DNA polymerase (Promega, Madison, WI, USA). Comparative semi quantitative PCR was performed as follows: GAPDH mRNA was first amplified at a low cycle number. If needed, cDNAs were adjusted to obtain similar intensities for GAPDH

signals with all the samples. The adjusted amounts of cDNA were subjected to PCR. The PCR conditions were an initial denaturation at 94°C for 2 min, denaturation at 94°C for 15 sec, annealing for 45 sec at the appropriate temperature and extension for 1 min at 72°C (24-33 cycles of amplification). Aliquots (15 µl) of the amplified cDNA were separated by 1.5% agarose gel electrophoresis. PCR products were separated on a 2% Nusieve (FMC Rockland, ME, USA, 3:1 agarose gel) and visualized by ethidium bromide staining under ultraviolet light.

Subcellular fractionation

Subcellular fractionation was done as described earlier with some modification [21]. In brief, RKO or HEK293 cells (1.2×106) were seeded into a 100 mm tissue culture plate. After AYPGKF activation (200 µM), cell media aspirated, washed (2X) with cold PBS, cells were lysed in 1 ml MES buffer (150 mM NaCl, 25 nM MES) supplemented with protease inhibitor cocktail, 1 mM phenylmethylsulfonylfluoride, PMSF, and 1 mM Na-orthovanadate (Sigma, St. Louis, MO, USA) to prevent protein degradation. Cell lysates were homogenized manually in a glass homogenizer (Wheaton, USA) using a B pestle (Wheaton, USA). Cell lysates were centrifuged at 1000× *g*/10 min at 4^{0}C. Supernatant (S1) was collected to isolate the cytoplasmic fraction and pellet (P1) was used to isolate the nuclear fraction. P1 was washed with MES buffer (2X) at 1000× *g*/10 min at 4^{0}C. The resultant pellet was resuspended in 200 µl NDG buffer (1% NP40, 0.5% Deoxycholic acid sodium salt (w/v), 10% glycerol in TBSpH 8.0). Pellet centrifuge at 16 000*g*/10min/4^{0}C, pellet again, washed with NDG buffer. The pellet obtained after centrifugation was suspended in 200 µl RIPA buffer and run-on gel as a nuclear fraction. Supernatant (S1) was centrifuged at 16 000×*g*/10 min/4^{0}C to remove contamination, and the received supernatant was transferred to a new tube and was ultra-centrifuged at 115 000× *g*/60 min/4^{0}C. The supernatant received after ultra-centrifugation was transferred to a new tube and used as a cytoplasmic fraction.

Cell lysate preparations, immunoprecipitation, and western blot

To prepare protein cell lysates for immunoprecipitation, cells were solubilized in CelLytic™ M buffer (Sigma-Aldrich, St. Louis, Mo, USA). Routinely, other protein cell lysate preparations contained: 10 mM Tris-HCl (pH 7.4), 150 mM NaCl, 1 mM EDTA, and 1% Triton X-100. All the lysis buffers mentioned were supplemented with a protease inhibitor cocktail, 1 mM phenylmethylsulfonylfluoride, PMSF, and 1 mM Na-orthovanadate (Sigma, St. Louis, MO, USA) to prevent protein degradation. Protein cell lysates used for IP and BA were incubated at 4^{0}C for 20 min and then disrupted by sonication. Finally, soluble supernatant was collected after centrifugation at 12 000 rpm for 20 min at 4^{0}C. Protein cell lysates were separated on 8%−10% SDS-PAGE followed by transfer to Immobilon-P membrane (Millipore, Bedford, MA, USA). Membranes were blocked and probed with the appropriate primary antibodies accordingly. Primary antibodies that include anti-flag (F3165; Sigma-Aldrich, USA), anti-β- actin (A5441; Sigma-Aldrich, St. Louis, Mo, USA), anti- β -catenin (C2206; Sigma-Aldrich, St. Louis, Mo, USA), anti-PAR_2 (AB180953; Abcam, USA:SC-13504 Santa Cruz), anti-HA (901503; Biolegend), anti-LRP6, were suspended in 3% BSA in 10 mM Tris−HCl pH 7.5, 100 mM NaCl and 0.1% Tween-20. After washes, blots were incubated with secondary antibodies conjugated to horseradish-peroxidase. Immunoreactive bands were detected by the enhanced chemiluminescence (ECL) reagent (Pierce, Rockford, IL, USA). Protein cell lysates (400−800 µg) were used for immunoprecipitation analysis. Anti PAR_2 (sc-13504; Santa Cruz), and anti PAR_4 antibodies (Abcam ab109174) were added to the cell lysates and processed as previously described [18].

TOP*flash* luciferase reporter assay

RKO or HEK 293 cells (0.2×106) were seeded in 6-well plates and incubated overnight at 37^{0}C. The cells were transfected with desired target plasmids (*Par2*, *Par4 gpr25*) along with human Lef-1 TOP*flash* (Tcf Optimal Promoter + luciferase), T cell factor (Tcf) reporter plasmid containing two sets (the second set in reverse orientation) of three copies of the Tcf binding site upstream of the thymidine kinase (TK) minimal promoter and luciferase open reading frame using PEI transfection reagent (Polysciences, Warrington, PA, USA). The CMV/β-gal plasmid was co-transfected as an internal control for transfection efficiency. After 48 h transfection, the cells were washed, lysed and then Luciferase assay was performed with the Luciferase Reporter System (Cat# E1500; Promega, Heidelberg, Germany) according to the manufacturer's instructions, and luminescence was detected on a Tecan SparkTM10M multimode microplate detection system (Switzerland).

Statistical analysis

All experiments were performed in triplicate, and data are presented as mean ± SEM. Statistical analyses were performed using Student's t-test or one-way or two-way analysis of variance (ANOVA), as appropriate, followed by multiple comparisons post hoc tests where applicable (GraphPad Prism 6.0). A P

value < 0.05 was considered statistically significant. Statistical significance is indicated as *P < 0.05, **P < 0.01, ***P < 0.001, ****P < 0.0001, and ns (not significant).

Results

PAR_4 induces β-catenin stabilization

Previously, we have demonstrated that PAR_2 stabilizes β-catenin levels [22]. This is similar with data obtained in our originally established line of transgenic mice directed to overexpress *Par1/f2r* in the mammary glands, exhibiting remarkably high levels of β-catenin [19]. Based on the notion that PAR_4 is a potent oncogene, capable effectively of inducing tumors in mice [18], we thought to examine whether it is also capable of stabilizing β-catenin levels (PAR3 serves as a co receptor). For this, HEK293 cells were transfected with *Par2, Par4* and *flag*-β-catenin plasmids, then activated for the indicated periods of time either with AYPGKF for PAR_4 activation or trypsin or SLIGKV for the activation of PAR_2. A significant increase in β-catenin levels was observed following PAR_4 activation as compared with PAR_2 induced β-catenin levels (Fig. 1A). While DVL is as an upstream cytoplasmic component centrally involved in the signaling of β-catenin stabilization, it is recognized that DVL exists also in the cell nucleus, where it acts as an essential component of the Wnt-β-catenin transcriptional complex. This depicts DVL a more complex role than initially thought. Its role as part of the transcriptional complex is found in addition to its task as being a scaffold protein bridging between seven transmembrane receptors and signaling components [23, 24]. To study whether PAR_4 can induce the translocation of DVL from the cytoplasm to the cell nuclei, HEK293 cells were transfected with *Par4* and *dvl* plasmids. Next, AYPGKF activation of PAR_4 was carried out, followed by the nuclear fraction isolation. As shown in Fig. 1B, abundant expression of DVL is observed in the nuclei following PAR_4 activation. Abundant DVL expression is observed 4–5 hours following AYPGKF activation. Nuclear fraction and protein loading are demonstrated by the housekeeping gene - lamin.

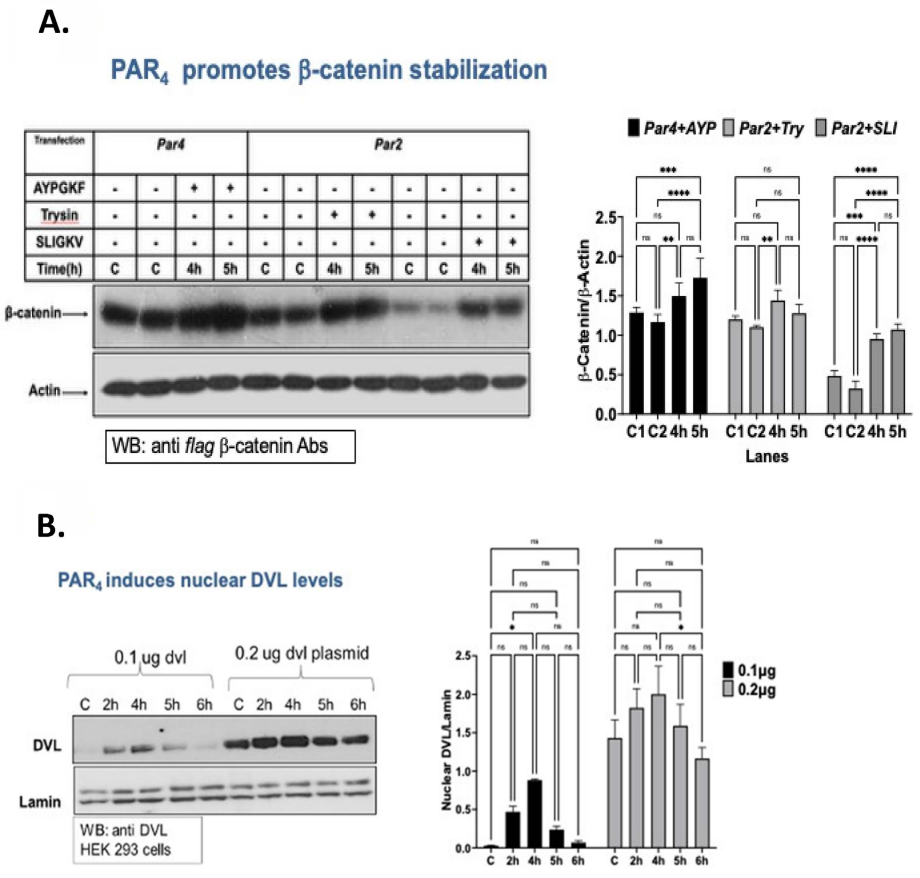

Figure 1: A. PAR_4 promotes β-catenin stabilization. HEK293 cells were transfected with *Par4* and *Par2* plasmids and with *flag*-β-catenin. Next, cells were activated for 4h and 5h with either AYPGKF for PAR_4 activation or SLIJGV or trypsin for PAR_2 activation. WB detection was carried out using anti-*flag* Abs. This is representative of three repeated independent experiments. **B. PAR_4 induces the translocation of cytoplasmic DVL to the cell nuclei.** HEK293 cells were transfected with *Par4* and *dvl* plasmids. Then, AYPGKF PAR_4 activations for 2h, 4h, 5h and 6h were carried out. Nuclear fraction was prepared and DVL was detected on WB using anti DVL Abs. Lamin was used as a housekeeping gene for loading nuclear proteins compartment. This is one of three independent experiments. A P value < 0.05 was considered statistically significant. Statistical significance is indicated as *P < 0.05, **P < 0.01, ***P < 0.001, ****P < 0.0001, and ns (not significant).

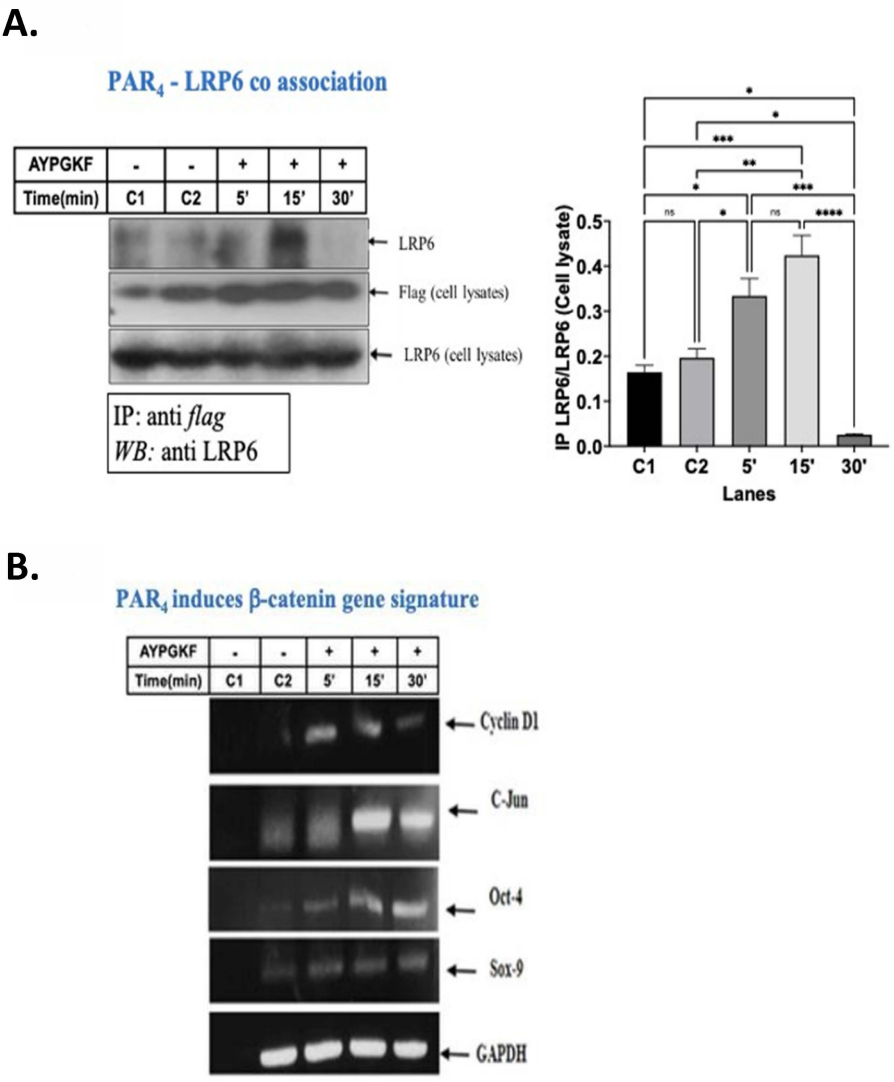

Figure 2: A. PAR$_4$ co associates with LRP6. HEK293 cells were transfected with *flag-Par4* and *lrp6* plasmids. Then AYPGKF PAR$_4$ activations were carried out for 5', 15' and 30' minutes followed by cell lysates preparation. IP was carried out by anti-*flag* Abs. WB detection was performed by anti LRP6 Abs. This experiment presents one out of three times performed. A P value < 0.05 was considered statistically significant. Statistical significance is indicated as *P < 0.05, **P < 0.01, ***P < 0.001, ****P < 0.0001, and ns (not significant). **B. PAR$_4$ induces β-catenin downstream target gene signature**. RKO cells were transfected with *Par4* plasmid and AYPGKF PAR$_4$ activated for 4, 6 and 8 hours. RNA was isolated and reverse transcribed to cDNA. β-catenin targets (e.g., cyclin D1, C-Jun, Oct-4 and Sox9) were analyzed by PCR and separated on 1% agarose gel. GAPDH was used as a housekeeping control gene for loading. This is representative of experiments performed.

LRP6 acts as a co receptor with PAR$_4$

LDL-receptor-related proteins 5 and 6; LRP5 and LRP6 are required receptors for the activation of β-catenin signaling in the canonical Wnt signaling pathway. Noticeably, while LRP5 and LRP6 exhibit high homology, they may not act in a comparable fashion to induce Wnt signals. LRP6 can induce autonomously axis duplication in Xenopus embryos, whereas LRP5 does not [25]. Deletion of LRP6 in mice is embryonically lethal, in contrast, LRP5- null mice are viable and fertile [26]. Therefore, we asked whether PAR$_4$ co associates with LRP6 while acting to stabilize β-catenin levels. HEK293 cells were transfected with *Par4* and *lrp6* plasmids, activated with AYPGKF for PAR$_4$ activation for the indicated time periods, followed by co-IP analysis. It is shown that activation of PAR$_4$ leads to the co association of LRP6 with PAR$_4$ as evident by the immunocomplex formed (Fig. 2A). Toward analysis of PAR$_4$ induced β-catenin transcriptional activity, we examined levels of selected β-catenin downstream target genes. RT-PCR analyses indicated that there is a significant increase in the levels of: cyclin D1, c-Jun, Oct 4 and Sox-9, following PAR$_4$ activation (Fig. 2B). Overall, activation of PAR$_4$ involves traditional steps in β-catenin stabilization, initially via the association with LRP6 co receptor, induced levels of nuclear DVL and enhanced β-catenin levels toward stimulated transcription of gene signature downstream.

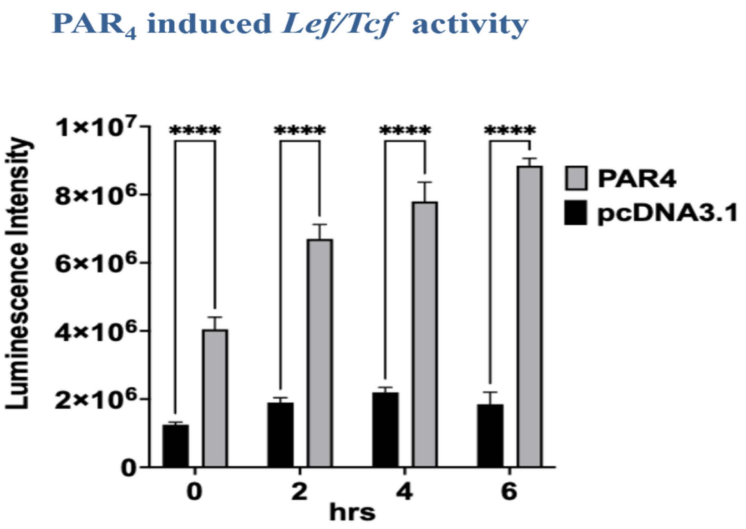

Figure 3: PAR_4-induced TOP*flash* transcriptional activity. TOP*flash* luciferase activity was analyzed in RKO cells following PAR_4 activation in the presence of *Par4* and *Lef*, *Tcf* constructs. The results were evaluated using GraphPad InStat software. Data are expressed as mean***p < .001. It represents one of three independent experiments performed in triplicates.

Induced TOP*flash* transcriptional activity by PAR_4

The transcriptional capability of PAR_4 induced β-catenin activity was evaluated using TOP*flash* luciferase activity. The experiments were performed on RKO colon carcinoma cells transfected with *Par4* along with plasmids of human Lef-1 TOP*flash* (Tcf Optimal Promoter + luciferase), T cell factor (Tcf) reporter plasmid of three copies of the Tcf binding site. Additionally, the CMV/β-gal plasmid was co-transfected, as an internal control for transfection efficiency. Cells were lysed, followed by luciferase assay determination using the Luciferase Reporter System (Cat# E1500; Promega, Heidelberg, Germany) according to the manufacturer's instructions. Luminescence detection indicated increased high *Lef/Tcf* response following AYPGKF PAR_4 activation for a period of 6 hours (Fig. 3).

PAR_4 co-associates with LGR5

Levels of PAR_2 (*f2rl1*) and PAR_4 (*f2rl3*) GPCRs are significantly elevated in CSC sphere formation and stem cell maintenance. This is based on transcriptome profile analysis survey of 195 cancer GPCRs that regulate the reprogramming of CSCs sphere formation [27]. While exploring prevailing candidate/s that may possibly associate with PAR_4, we evaluated the option of LGR5, a known cancer stem cell marker as a principal candidate for the interaction with PAR_4. Based on the potent co association of PAR_2 with LGR5 [20], we wondered whether there is a common theme shared within PAR family members and thought whether PAR_4 is also a potential co-partner associating with LGR5. As studied for PAR_2, the dominant member among the PAR family [18, 28, 29], immunoprecipitation analyses between LGR5 and PAR_4, were carried out. It is demonstrated that PAR_4 co associates with LGR5 (Fig. 4A). In-parallel, we performed protein-protein docking using software (such as AF3 using the HADDOCKv2.4 server), and various parameters (interactions; via hydrophobic contacts, van der Waals interactions and ionic bonds; energy; via PDBePISA analysis) indicate that both (LGR5 and PAR_4) (Fig. 4B) indeed have the potential to form a stable complex (supplementary data Tables S1 & S2). With respect to the docking of protein-protein analyses, increased number of studies have demonstrated the presence of homo-, heterodimers and even oligomers following between two or more GPCR associations [30]. Advanced fluorescence methods such as fluorescence resonance energy transfer (FRET) or bioluminescence resonance energy transfer (BRET) as also Docking Assay For Transmembrane Components (DAFT) assays that enable the measure aggregation of GPCRs concurrently assisted in establishing GPCR heterodimer formation [31]. Overall, these techniques clearly indicated that for dimerization to occur, the GPCR transmembrane domains come together through lateral diffusion within the lipid bilayer [32, 33]. This is demonstrated here for PAR_4-LGR5 interactions (Fig. 4B).

GPR25 induces β-catenin stabilization

GPR25 is a poorly studied GPCR of seven transmembrane domains of unidentified functions. GPR25 was found in 1997 [34] and was considered an orphan receptor of an unknown ligand. When we screened GPR25 expression in a wide panel of cell lines

representing different types of epithelial cancers such; breast, lung, ovary, colon and pancreas, the following results were obtained. RT-PCR analyses showed the selective expression of GPR25 in cancers of the GI (Fig. 5). Based on its expression in cells of the GI system, GPR25 was selected to further study its potential activation of β-catenin process. When we asked whether activation (in the presence of 10% serum) of GPR25 can induce β-catenin stabilization, it was found that high levels of β-catenin were obtained (Fig. 6A). This was observed in HEK293 cells transfected with *gpr25* and *flg*-β-catenin plasmids, followed by activation for the indicated time periods. Along with this line of evidence, consistently increased response of TOPflash (*Lef/Tcf*) luminescence indicative of β-catenin transcriptional activity was obtained in the presence of activated GPR25 (Fig. 6B). As GPR25 strongly induces β-catenin stabilization the potential co association with LGR5 was raised. Indeed, GPR25 was found as a co-partner of LGR5 forming a joint immunocomplex (Fig. 7). *Protein-protein* docking analysis using AlphaFold 3 and HADDOCKv2.4 server, as also PDBePISA analyses confirmed the binding association between GPR25 and LGR5. Overall, co association with LGR5 was found for FZD receptors [14], PAR_2 [20], PAR_4 and GPR25 all which co associate with LGR5. Our data was assessed both by co immunoprecipitations and *protein-protein* docking analyses.

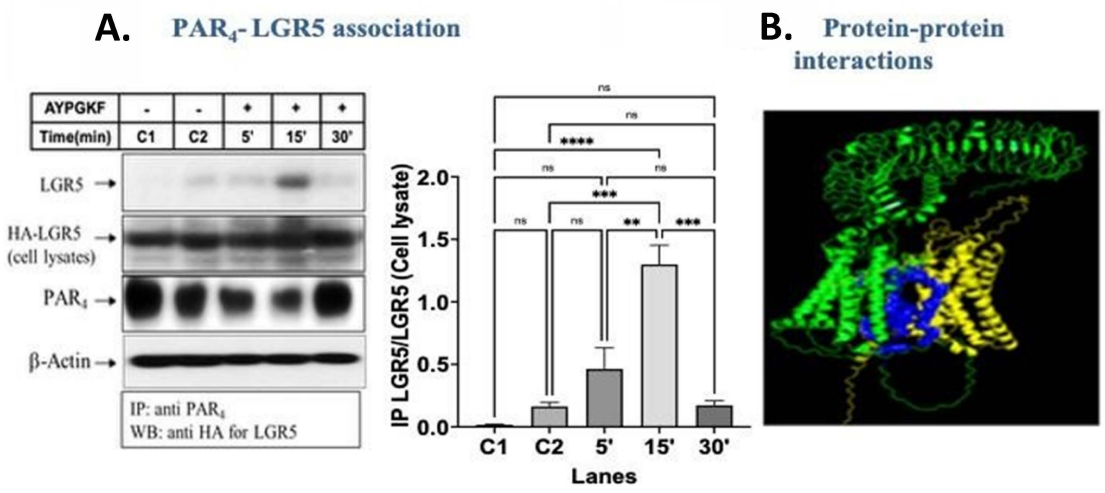

Figure 4: PAR_4-associated LGR5. **Left**. PAR_4-LGR5 complex formation. PAR_4 forms a complex with LGR5 following AYPGKF PAR_4 activation. **Right**. **Protein-protein docking**. PAR_4 (yellow) and LGR5 (green) interaction were predicted using AlphaFold 3 and HADDOCKv2.4. The blue region represents predicted interface between the two proteins.

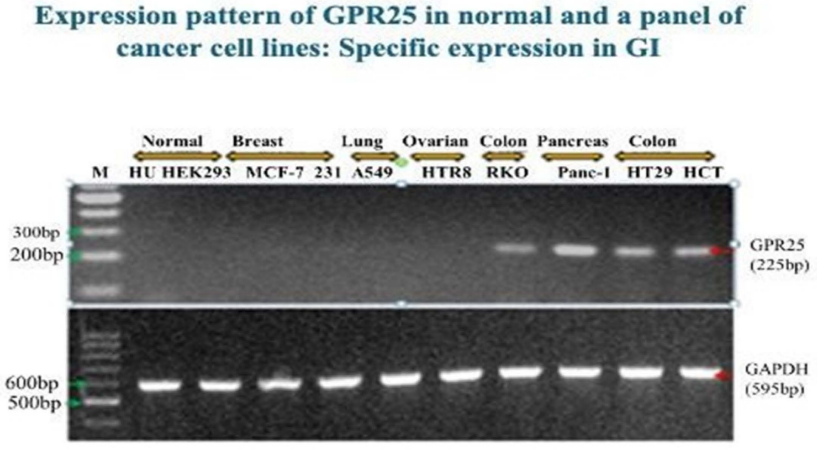

Figure 5: RT-PCR of *gpr25* in established cancer cell lines. Levels of GPR25 in various cancer cell lines of different origins. RT-PCR analysis was carried out in RNA isolated from these established cell lines of different origins. GAPDH was used as housekeeping control gene.

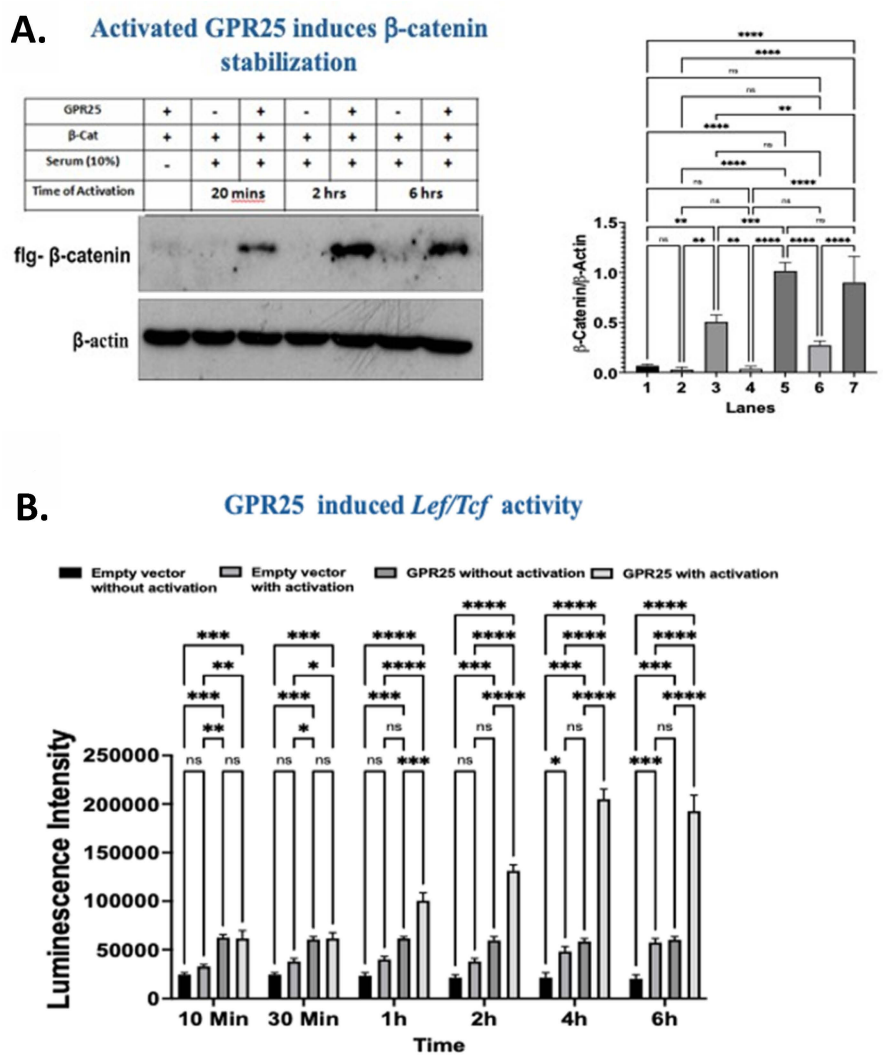

Figure 6: A. Stabilization of β-catenin in the presence of GPR25. HEK293 cells were transfected with *flg* - β -catenin and *gpr25*. Levels of β-catenin were detected in thepresence and absence of *gpr25* and 10% serum for activation. This is one of three times repeated experiment. **Fig. 6B:** *Lef/Tcf* activity in the presence of GPR25. Enhanced *Lef/Tcf* transcriptional activity in the presence of *gpr25* plasmid transfected HEK293 cells, activated by 10% serum. Data are expressed as mean***$p < .001$. This is one out of three experiments performed in triplicates.

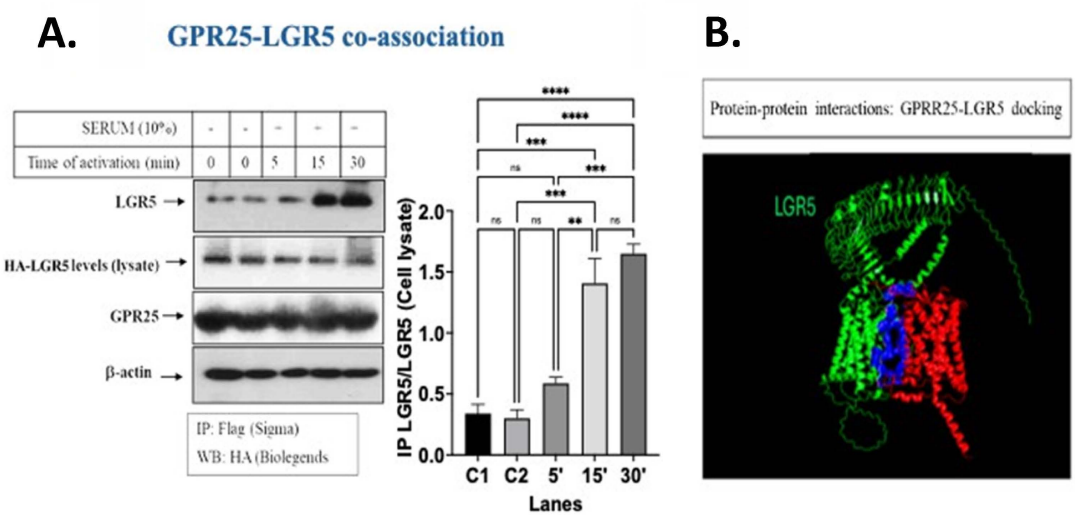

Figure 7: LGR5-GPR25 co association. Left. HEK293 were transfected with *lgr5* and *GPR25*. IP was carried out showing specific co-association after 15 and 30 min of 10% serum for activation. This was shown per input of equal levels of LGR5 and GPR25. **Right.** Protein-protein docking. Interactions between GPR25 (red) with LGR5 (green) were determined using Alpha Fold3, SWISS-MODEL and HANDDOCK v2.4 protein–protein docking server. The blue region highlights the predicted interaction interface between the two proteins.

Discussion

Here we demonstrate that PAR_4 and GPR25, both cancer GPCRs, potently induce β-catenin stabilization and co associate with LGR5 of stem cell properties. We focus on colon cancer whereby GPR25 is highly expressed (Fig. 5). PAR_4 was shown earlier as highly expressed in colon cancer cell lines [35] as well as in colon cancer tissue sections [36], absent in the nearby normal colonic epithelial cells. PAR_4 has been demonstrated also expressed in organoids isolated from fresh intestinal crypts, grown and maintained as three-dimension spheres [18, 37]. In fact, organoids provide a good experimental system for cancerous tissues [38], recapitulating the entire colonic tumor tissue cell population. Overall, based on organoid culture studies on one hand and bioinformatic transcriptional outline of selected GPCRs on the other [39], it is suggested that PAR_4/*f2rl3* plays a role in the colon stem cell progenitor niche. Furthermore, PAR_4 has been shown involved in a wide panel of epithelial malignancies [18, 40-43]. GPR25 is a poorly characterized GPCR. GPR25 has long been thought to be an orphan receptor with no known endogenous ligand. However, a recent publication indicated that C-X-C chemokine 17 (CXCL17), functions as a ligand for GPR25 and mediates lymphocyte homing [44]. In addition, GPR25 as a member of GPCR class A sub class has been also shown to have a ligand-independent constitutive activity [45]. Here, we provide evidence that the two cancer GPCRs; PAR4 and GPR25 both of which are involved in colon cancer, are capable of potently induce the β-catenin stabilization process and powerfully associate with LGR5. Consequences of this co-association between PAR_4 or GPR25 with LGR5 remain yet to be fully studied. Nonetheless, the implication of GPR25 association with LGR5 and as a potent inducer of β-catenin stabilization is that it may potentially serve as a target of cancer therapy. LRP6 is a well characterized co-receptor in cancer β-catenin stabilization process. Classically, LRP6 singalosome is formed following Wnt ligation to both FZDs and LRP6 which recruits DVL to the cell membrane. This is followed by DVL binding to AXIN-GSK3β-CK1α that leads to phosphorylation of the serine residue within PPPSP motif in the cytoplasmic tail of LRP6. GSK3β and CK1α kinases mediate the phosphorylation of LRP6 and the dissociation of the β-catenin from the "destruction complex". This leads to stabilized β-catenin that enters the cell nuclei and associates with *Lef/Tcf* transcription factors to induce the levels of a target genes signature [46, 47]. We show that PAR_4 co-associates with LRP6, as was previously shown for $PAR_{1\&2}$ PAR family members [22, 48]. DVL is a pivotal hub protein traditionally communicating cues from Wnts ligation to FZDs and LRP6 receptors [49, 50]. While historically the cytoplasmic role of DVL as a scaffold Wnt signal component was the center of research [51-53] its nuclear role as part of a transcription complex has become evident [54, 55]. It has been shown that alteration of DVL1 expression has an impact on the transcriptomic landscape enabling the mapping of DVL binding sites to promoters of target genes [56]. Among the known transcription factors that are associated with nuclear DVL are FOXK1 and FOXK2 [57]), ETS1 [54] and CYP19A1 [58] as well as control of immunomodulatory genes [59].

Conclusions

Cancer driver GPCRs; PAR_2 [20], PAR_4 and GPR25 are co assembled with LGR5 as judged by co immunoprecipitation analyses and *protein-protein* docking evaluations. These GPCR receptors effectively elicit β-catenin stabilization and are possibly involved in CSCs regulation. It may nonetheless open new directions for therapeutic interventions.

Abbreviations

CSCs: Cancer stem cells; PARs: Protease activated receptors; GPCRs: G-protein coupled receptors; LGR5: Leucine rich- repeat G-protein coupled receptor 5; GPR25: G-protein coupled receptor 25; DVL: Dishevelled; LRP6: Low-Density Lipoprotein Receptor Related 6; FZD: Frizzled; sFRP: secreted Frizzled Related Protein; RNF43: Ring Finger protein 43; GI: Gastrointestinal.

Supplementary Material

Supplementary tables.
https://www.jcancer.org/v17p1408s1.pdf

Acknowledgements

We thank members of the Bar-Shavit R laboratory for contributing to stimulating discussions on GPCR sand cancer stem cell niche.

Competing Interests

The authors have declared that no competing interest exists.

References

1. Batlle E, Clevers H. Cancer stem cells revisited. Nat Med. 2017; 23(10): 1124-1134.
2. Agudo J, Miao Y. Stemness in solid malignancies: coping with immune attack. Nat Rev Cancer. 2025; 25(1): 27-40.
3. Fumagalli A, Oost CC, Kester L, Morgner J, Bornes L, et al. Plasticity of Lgr5-Negative Cancer Cells Drives Metastasis in Colorectal Cancer. Cell Stem Cell. 2020; 26(4): 569-578.
4. Ogden S, Metic N, Leylek O, Smith EA, Berner AM, et al. Phenotypic heterogeneity and plasticity in colorectal cancer metastasis. Cell Genom. 2025; 5(7):100881-100893.

5. Vermeulen L, De Sousa EMF, van der Heijden M, Cameron K, de Jong JH, Borovski T, Tuynman JB, Todaro M, Merz C, Rodermond H, Sprick MR, Kemper K, Richel DJ, Stassi G, Medema JP. Wnt activity defines colon cancer stem cells and is regulated by the microenvironment. Nat Cell Biol. 2010; 12: 468-476.
6. de Sousa EMF, Kurtova AV, Harnoss JM, Kljavin N, Hoeck JD, Hung J, Anderson J, Storm EEE, Modrusan Z, Koeppen H, Dijkgraaf GJ, Piskol R, de Sauvage FJA. distinct role for Lgr5(+) stem cells in primary and metastatic colon cancer. Nature. 2017; 543: 676-680.
7. Shimokawa M, Ohta Y, Nishikori S, Matano M, Takano A, Fujii M, Date S, Sugimoto S, Kanai T, Sato T. Visualization and targeting of LGR5(+) human colon cancer stem cells. Nature. 2017; 545:187-192.
8. Lenos KJ, Miedema DM, Lodestijn SC, Nijman LE, van den Bosch T, Romero RX, Lourenco FC, Lecca MC, van der Heijden M, van Neerven SM, van Oort A, Leveille N, Adam RS, de Sousa EMF, Otten J, Veerman P, Hypolite G, Koen SL, Lyons SK, Stassi G, Winton DJ, Medema JP, Morrissey E, Bijlsma MF, Vermeulen L. Stem cell functionality is microenvironmentally defined during tumor expansion and therapy response in colon cancer. Nat Cell Biol. 2018; 20: 1193-1202.
9. Pawar NR, Buzza MS, Antalis TM. Membrane-anchored serine proteases and protease-activated receptor-2-mediated signaling: Co-conspirators in cancer progression. Canc Res. 2019; 79: 301-310.
10. Plaks V, Kong N, Werb Z. The cancer stem cell niche: how essential is the niche in regulating stemness of tumor cells? Cell Stem Cell. 2015; 16: 225-238.
11. Barker N, Clevers H. Catenins, Wnt signaling and cancer. Bioessays. 2000; 22(11): 961-5, Review.
12. van de Wetering M, Sancho E, Verweij C, de Lau W, Oving I, et al. The beta-catenin/TCF-4 complex imposes a crypt progenitor phenotype on colorectal cancer cells. Cell. 2002; 111(2): 241-50.
13. Van der Flier LG, Sabates-Bellver J, Oving I, Haegebarth A, De Palo M, et al. The Intestinal Wnt/TCF Signature. Gastroenterology. 2007; 132(2): 628-632.
14. de Lau W, Barker N, Low TY, Koo B-K, Li VSW, et al. Lgr5 homologues associate with Wnt receptors and mediate R-spondin signalling. Nature. 2011; 476: 293-297.
15. Glinka A, Dolde C, Kirsch N, Huang Y-L, Kazanskaya O, et al. LGR4 and LGR5 are R-spondin receptors mediating Wnt/-catenin and Wnt/PCP signalling. EMBO Rep. 2011; 12: 1055-1061.
16. Ma Y, He L, Zhao X, Li W, Lv X, Zhang X, Peng J, Yang L, Xu Q, Hongying Wang H. Protease activated receptor 2 signaling promotes self-renewal and metastasis in colorectal cancer through β-catenin and periostin. Cancer Lett. 2021; 521:130-141.
17. Kancharla A, Maoz M, Jaber M, Agranovich D, Peretz T, Grisaru-Granovsky S, Uziely B, Bar-Shavit R. PH motifs in PAR1&2 endow breast cancer growth. Nat Commun. 2015; 6: 8853- 8863.
18. Nag JK, Malka H, Sedley S, Appasamy P, Rudina T, Levi T, Hoffman A, Gilon C, Uziely B, Bar-Shavit R. PH-Binding Motif in PAR4 Oncogene: From Molecular Mechanism to Drug Design. Molecular Cancer Therapeutics. Mol Cancer Ther. 2022; 21:1415-1429.
19. Yin YJ, Katz V, Salah Z, et al. Mammary gland tissue targeted overexpression of human protease-activated receptor 1 reveals a novel link to beta-catenin stabilization. Cancer Res. 2006; 66: 5224-5233.
20. Nag JK, Appasamy P, Sedley S, Malka H, Rudina T, Bar-Shavit R. RNF43 induces the turnover of protease-activated receptor 2 in colon cancer. FASEB J. 2023; 37(1): e22675-22697.
21. German CL, Howe CL. Preparation of biologically active subcellular fractions using the Balch homogenizer. Anal Biochem. 2009; 394: 117-124.
22. Nag JK, Kancharla A, Maoz M, Turm H, Agranovich D, Gupta CL, Uziely B, Bar-Shavit R. Low-density lipoprotein receptor-related protein 6 is a novel coreceptor of protease-activated receptor-2 in the dynamics of cancer-associated β-catenin stabilization. Oncotarget. 2017; 8(24): 38650-38667.
23. Itoh K, Brott BK, Bae GU, Ratcliffe MJ, Sokol SY. Nuclear localization is required for Dishevelled function in Wnt/ beta-catenin signaling. Journal of biology. 2005; 4: 3-9.
24. Torres MA, Nelson WJ. Colocalization and redistribution of dishevelled and acting during Wnt-induced mesenchymal morphogenesis. The Journal of cell biology. 2000; 149:1433-1442.
25. Tamai K, Semenov M, Kato Y, Spokony R, Liu C, Katsuyama Y, Hess F, Saint-Jeannet JP, He X. LDL-receptor-related proteins in Wnt signal transduction. Nature. 2000; 407:530-535.
26. Pinso KI, Brennan J, Monkley S, Avery BJ, Skarnes WC. An LDL-receptor-related protein mediates Wnt signalling in mice. Nature. 2000; 407:535-538.
27. Choi HY, Saha SK, Kim K, et al. G protein-coupled receptors in stem cell maintenance and somatic reprogramming to pluripotent or cancer stem cells. BMB Rep. 2015; 48: 68-80.
28. Jaber M, Maoz M, Kancharla A, et al. Protease-activated- receptor-2 affects protease-activated- receptor- 1-driven breast cancer. Cell Mol Life Sci. 2014; 71: 2517-2533.
29. Sevigny LM, Austin KM, Zhang P, et al. Protease-activated receptor-2 modulates protease-activated receptor-1-driven neointimal hyperplasia. Arterioscler Thromb Vasc Biol. 2011; 31: e100-e106.
30. Gahbauer S, Böckmann RA. Membrane-Mediated Oligomerization of G Protein Coupled Receptors and Its Implications for GPCR Function. Front Physiol. 2016; 7: 494-511.
31. Pluhackova K, Böckmann RA. Biomembranes in atomistic and coarse-grained simulations. J Phys Condens Matter. 2015; 27: 323103-32118.
32. Maggio R, Fasciani I, Carli M, Petragnano F, Marampon F, Rossi M, Scarselli M. Integration and Spatial Organization of Signaling by G Protein-Coupled Receptor Homo- and Heterodimers. Biomolecules. 2021; 11(12):1828-1834, Review.
33. Wouters E, Marín AR, Dalton JAR, Giraldo J, Stove C. Distinct Dopamine D_2 Receptor Antagonists Differentially Impact D_2 Receptor Oligomerization. Int J Mol Sci. 2019; 20(7): 1686-1711.
34. Jung BP, Nguyen T, Kolakowski LF Jr, Lynch KR, Heng HHQ, George SR, Brian F, O'Dowd BF. Discovery of a Novel Human G Protein-Coupled Receptor Gene (GPR25) Located on Chromosome 1. Biochemical and Biophysical Research Communications. 1997; 230: 69-72.
35. Gratio V, Walker F, Lehy T, Labarthe M, Darmoul D. Aberrant expression of proteinase-activated receptor 4 promotes colon cancer cell proliferation through a persistent signaling that involves Src and ErbB-2 kinase. Int J Cancer. 2009; 124:1517–1525.
36. Yu G, Jiang P, Xiang Y, et al. Increased expression of protease-activated receptor 4 and Trefoil factor 2 in human colorectal cancer. PLoS One. 2015;10(4):e0122678.
37. Ando S, Otani H, Yagi Y, Kawai K, Araki H, Fukuhara S, Inagaki C. Proteinase-activated receptor 4 stimulation-induced epithelial-mesenchymal transition in alveolar cells. Respir Res. 2007; 8: 31–45.
38. Kaufmann R, Rahn S, Pollrich K, Hertel J, Dittmar Y, Hommann M, Henklein P, Biskup C, Westermann M, Hollenberg MD, et al. Thrombin-mediated hepatocellular carcinoma cell migration: Cooperative action via proteinase-activated receptors 1 and 4. J Cell Physiol. 2007; 211: 699–707.
39. Hurevich M, Swed A, Joubran S, Cohen S, Freeman NS, Britan-Rosich E, Briant-Longuet L, Bardy M, Devaux C, Kotler M, et al. Rational conversion of noncontinuous active region in proteins into a small orally bioavailablemacrocyclic drug-like molecule: The HIV-1 CD4:Gp120 paradigm. Bioorg Med Chem. 2010; 18:5754–5761.
40. Yu G, Jiang P, Xiang Y, Zhang Y, Zhu Z, Zhang C, Lee S, Lee W, Zhang Y. Increased expression of protease-activated receptor 4 and Trefoil factor 2 in human colorectal cancer. PLoS One. 2015; 10: e0122678.
41. Wilson SR, Gallagher S, Warpeha K, Hawthorne SJ. Amplification of MMP-2 and MMP-9 production by prostate cancer cell lines via activation of protease activated receptors. Prostate. 2004; 60: 168–174.
42. Musbach F, Henklein P, Westermann M, Settmacher U, Bohmer FD, Kaufmann R. Proteinase-activated receptor 1- and 4-promoted migration of Hep3B hepatocellular carcinoma cells depends on ROS formation and RTK transactivation. J Cancer Res Clin Oncol. 2015; 141: 813–825.
43. Elste AP, Petersen I. Expression of proteinase-activated receptor 1-4 (PAR 1-4) in human cancer. J Mol Histol. 2010; 41: 89–99.
44. Ocon B, Xiang M, Bi Y, Tan S, Brulois K, Ayesha A, Kunte M, Zhou C, LaJevic M, Lazarus N, Mengoni F, Sharma T, Montgomery S, Hooper JE, Huang M, Handel T, Dawson JRD, Kufareva I, Zabel BA, Pan J, Butcher EC. A lymphocyte chemoaffinity axis for lung, non-intestinal mucosae and CNS. Nature. 2024; 635(8039): 736-745.
45. Martin AL, Steurer MA, Aronstam RS. Constitutive Activity among Orphan Class-A G Protein Coupled Receptors. PLoS One. 2015; 10: e0138463.
46. Nusse R, Clevers H. Wnt/beta-catenin signaling, disease, and emerging therapeutic modalities. Cell. 2017; 169:985-99.
47. Zhan T, Rindtorff N, Boutros M. Wnt signaling in cancer. Oncogene. 2017; 36:1461-73.
48. Grisaru-Granovsky S, Kumar Nag J, Zakar L, Rudina T, Lal Gupta C, Maoz M, Kozlova D, Bar-Shavit R. PAR1&2 driven placenta EVT invasion act via LRP5/6 as coreceptors. FASEB J. 2020; 34(12):15701-15717.
49. Gao C, Chen YG. Dishevelled: The hub of Wnt signaling. Cell Signal. 2010; 22: 717-727
50. Ma W, et al. Single-molecule dynamics of Dishevelled at the plasma membrane and Wnt pathway activation. Proc Natl Acad Sci USA. 2020; 117: 16690-16701.
51. Bilić J, Huang Y-L, Davidson G, et al. Wnt induces LRP6 signalosomes and promotes Dishevelled-dependent LRP6 phosphorylation. Science. 2007; 316: 1619-1622.
52. Fiedler M, Mendoza-Topaz C, Rutherford TJ, Mieszczanek J, Bienz M. Dishevelled interacts with the DIX domain polymerization interface of Axin to interfere with its function in downregulating β-catenin. Proc Natl Acad Sci USA. 2011; 108: 1937–1942.
53. Schwarz-Romond T, et al. The DIX domain of Dishevelled confers Wnt signaling by dynamic polymerization. Nat Struct Mol Biol. 2007; 14: 484-492.
54. Itoh K, Brott BK, Bae GU, Ratcliffe MJ, Sokol SY. Nuclear localization is required for Dishevelled function in Wnt/beta-catenin signaling. J Biol. 2005; 4: 3e1-12.
55. Sharma M, Molehin D, Castro-Piedras I, Martinez EG, Pruitt K. Acetylation of conserved DVL-1 lysines regulates its nuclear translocation and binding to gene promoters in triple-negative breast cancer. Sci Rep. 2019; 9: 16257e1-15.
56. Martinez-Marin D, Sharma M, van Wunnik JC, de Miranda FS, Boligala GP, Jull EC, Stroman GC, Babcock RL, Pruitt K. Dishevelled-1 regulates global transcriptomic changes and associates with ETS1 transcription factor. Nat Commun. 2025;16(1):6288e1-12.
57. Wang W, Li X, p Lee M, et al. FOXKs promote Wnt/β-catenin signaling by translocating DVL into the nucleus. Dev Cell. 2015; 32: 707-718.
58. Castro-Piedras I, Sharma M, Meghan den BakkerM, Deborah Molehin D, et al. DVL1 and DVL3 differentially localize to CYP19A1 promoters and regulate aromatase mRNA in breast cancer cells. Oncotarget. 2018; 9: 35639- 35654.

59. Sharma M, Castro-Piedras I, Rodgers AD, Pruitt K. Genomic profiling of DVL-1 and its nuclear role as a transcriptional regulation triple negative breast cancer. Genes Cancer. 2021; 12: 77-95.